Progress In Electromagnetics Research B, Vol. 62, 241–253, 2015

Antenna Correlation and Its Impact on Multi-Antenna System

Xiaoming Chen*

Abstract—It is generally believed that antenna correlations of up to 0.5 in magnitude have negligible effects on the performance of multi-antenna systems, and that antenna correlation only affects the system performance via its magnitude. In this paper, we show that antenna correlations of 0.5 in magnitude that has negligible effect in capacity (i.e., theoretically maximum data rate) can cause noticeable degradation on the throughput (i.e., actual achievable data rate); and that, when the number of antennas is larger than two, the phase of the correlation also has an impact on the performance of multi-antenna system. We demonstrated these via simulations and measurements in a reverberation chamber.

1. INTRODUCTION

Due to its high spectral efficiency, multiple-input multiple-output (MIMO) system has received enormous attentions and found applications in many modern wireless systems (e.g., long term evolution (LTE) and wireless local area network (WLAN)) over the past decade. One of the practical limiting factors of the MIMO system is the correlations between antennas at the transmitter and/or receiver. Take the cellular system for example: antennas at the base station (BS) usually experience high correlation due to limited angular spread resulting from sparse scatters around the BS; whereas the mobile station (MS) also suffers from correlations due to limited space in the mobile terminal. The correlations seen at the antenna ports (i.e., antenna correlations) are the combined effects of the channel and the antennas. This work is devoted to studying antenna correlations and their effects on the performances of multi-antenna systems.

It is commonly believed in the literature that a correlation of up to 0.5 in magnitude is negligible for the performance of multi-antenna system, e.g., [1], and that the correlation affects the MIMO performances only via its magnitude, e.g., [2]. In this paper, however, we show that the antenna correlations (even with small magnitudes) can have a noticeable adverse effect on the MIMO throughput. We also show that for a two-port antenna, the correlation affects the MIMO performance only via its magnitude, whereas for antennas with more than two ports, the phases of the correlations also affect the MIMO performance. We demonstrate these both theoretically and experimentally via simulations and measurements.

The work has been partially presented in a conference paper [3]. In this work, we extend the paper with different correlation models and analyses of their feasibilities (i.e., the positive semidefiniteness of the resulting correlation matrices); we also include new performance metric and new measurements in a reverberation chamber (e.g., [4]) for further demonstrating the correlations' effects.

2. ANTENNA CORRELATION

Based on the considered random variables [e.g., (equivalent baseband) signal, signal envelope, and signal power], there are three types of correlations in the literature, namely, signal correlation, envelope

Received 28 January 2015, Accepted 16 March 2015, Scheduled 20 March 2015
* Corresponding author: Xiaoming Chen (xiaoming.chen@qamcom.se).
The author is with the Qamcom Research & Technology, Gothenburg 412 85, Sweden.

correlation, and power correlation. The correlation between two signals at the mth and nth antenna ports, X_m and X_n, is given according to the definition of correlation coefficient [5]

$$\rho_{mn} = \frac{E\left[\left(X_m - E[X_m]\right)\left(X_n - E[X_n]\right)^*\right]}{\sqrt{E\left[\left|X_m - E[X_m]\right|^2\right] E\left[\left|X_n - E[X_n]\right|^2\right]}} \tag{1}$$

where E represents the expectation operator, and the superscript $*$ denotes complex conjugate. Envelop and power correlations are obtained by replacing X_i in (1) with $|X_i|$ and $|X_i|^2$ ($i = m, n$), respectively. It is shown that the power correlation is equal to the magnitude square of the signal correlation, and approximately equal to the envelope correlation [6]. We focus on the signal correlation in the sequel of the paper.

By approximating the expectation with sample mean, (1) can be used for estimating antenna correlations when the channel samples are obtained from, e.g., reverberation chamber (RC) measurements [7]. From the antenna point of view, there is a more tractable method for calculating antenna correlation. It is given as [8]

$$\rho_{mn} = \frac{\iint\limits_{4\pi} \mathbf{g}_m^H(\Omega)\mathbf{P}_{inc}(\Omega)\mathbf{g}_n(\Omega)d\Omega}{\sqrt{\iint\limits_{4\pi} \mathbf{g}_m^H(\Omega)\mathbf{P}_{inc}(\Omega)\mathbf{g}_m(\Omega)d\Omega \cdot \iint\limits_{4\pi} \mathbf{g}_n^H(\Omega)\mathbf{P}_{inc}(\Omega)\mathbf{g}_n(\Omega)d\Omega}} \tag{2}$$

where Ω denotes the solid angle; $\mathbf{g}_i$ is the embedded far field function (a column vector with elements representing for different polarizations) at the ith antenna port; the superscript H represents the Hermitian operator (i.e., conjugate transpose); $\mathbf{P}_{inc}$ stands for the dyadic power angular spectrum of the incident waves.

Once the antenna correlations are known, the correlation matrix at the N-port antenna can be constructed as

$$\mathbf{\Phi} = \begin{bmatrix} 1 & \rho_{12} & \cdots & \rho_{1N} \\ \rho_{12}^* & 1 & \cdots & \rho_{2N} \\ \vdots & \vdots & \ddots & \vdots \\ \rho_{1N}^* & \rho_{2N}^* & \cdots & 1 \end{bmatrix}. \tag{3}$$

Note that in polarization-balanced isotropic scattering environments, e.g., a well-stirred RC, $\mathbf{P}_{inc}(\Omega) = \mathbf{I}$. The resulting spatial correlation (without antenna effect) becomes a deterministic (sinc) function of the antenna separation (see Appendix A) and the antenna correlation can be determined from the antenna characteristics alone. Equation (2) shows the antenna correlation can be calculated from the (embedded) antenna patterns, whereas Blanch et al. [9] showed that the antenna correlation can be equivalently calculated from its S-parameters (provided that the Ohmic loss in the antenna is negligible). The S-parameter based correlation expression in [9] is for the envelop correlation for two-port antennas. The S-parameter based correlation is extended to the lossy antenna case and expressed for signal correlation in [10]. Nevertheless, since the main purpose of this paper is to investigate the impact of antenna correlations on multi-antenna systems, for practical antennas, it is suffice to use the more general correlation Expressions (1) and/or (2).

3. CORRELATION MODELS

For the convenience of analysis and without confining to specific antennas, it is common in the literature to assume a simplified correlation model for MIMO performance evaluations, e.g., [11, 12]. We discuss several correlation models in this section.

Correlation matrices consisting of antenna correlations calculated using (1) or (2) from measured or simulated channel samples are undoubtedly physical (or feasible). Using the jargons of matrix theory and statistics, they are positive semidefinite [13] almost surely [5]. However, correlation matrices constructed from correlation models may not necessarily be positive semidefinite. Therefore, we ought to check the feasibility of each correlation model.

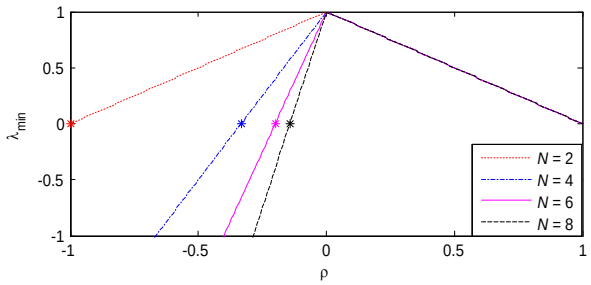

Figure 1. Minimum eigenvalues of correlation matrices as function of uniform correlation. The asterisk points are $(-1/(N-1), 0)$ for different N values.

3.1. Uniform Correlation

Arguably the simplest correlation model is uniform correlation,

$$\rho_{mn} = \rho. \tag{4}$$

Although this model may seem too simple to be realistic, it does result in useful conclusions under certain circumstances for system evaluation. Moreover, some practical multi-port antennas indeed have uniform correlations (e.g., see Figure 3 in [14]).

To satisfy the Hermitian property of the correlation matrix, i.e., $\mathbf{\Phi} = \mathbf{\Phi}^H$, ρ in (4) has to be real-valued. Thus, the correlation phase effect of the uniform correlation model can only be studied using positive- and negative-valued ρ. Furthermore, for the feasibility of the resulting correlation matrix, i.e., for $\mathbf{\Phi}$ to be positive semidefinite, ρ must be no smaller than $-1/(N-1)$. (See Appendix B for a proof of this).

To illustrate fact that ρ must be no smaller than $-1/(N-1)$ for $\mathbf{\Phi}$ to be feasible, we calculated the minimum eigenvalues as a function ρ for different N values and plotted them in Figure 1, where the asterisk points are $(-1/(N-1), 0)$ for different N values. According to matrix theory, $\mathbf{\Phi}$ is positive semidefinite if all its eigenvalues are nonnegative (i.e., its smallest eigenvalue should be larger than or equal to zero). As can be seen from Figure 1, for all the N values, the correlation matrix becomes positive semidefinite when

$$\rho \geq -1/(N-1). \tag{5}$$

3.2. Exponential Correlation

The exponential correlation [11, 12] is a popular correlation model in the communications society. It is given as

$$\rho_{mn} = \exp\left(-\frac{x_{mn}}{x_0}\right) \tag{6}$$

where x_{mn} is the distance between the mth and nth antenna elements and x_0 the decorrelation distance (at which the correlation reduces to $1/e$). Clearly, the correlation value depends on both x_{mn} and x_0. For a fixed x_0, the correlation decreases with increasing antenna separation x_{mn}; for a fixed x_{mn}, the correlation increases with increasing x_0. For a BS located well above the roof, x_0 can be up to dozens of wavelength; whereas for a MS in dense urban scenario, x_0 is around half-wavelength [15]. The fact that the correlation matrix constructed from (3) is positive semidefinite can be readily proved based on Theorem 2 in [16].

3.3. Bessel Correlation

Perhaps a more plausible correlation model is zeroth order Bessel function of the first kind [15],

$$\rho_{mn} = J_0\left(kx_{mn}\right) \tag{7}$$

where k is wave number. It can be readily derived as the spatial correlation in a two-dimension (2-D) uniform scattering environment (by following the same lines in Appendix A for 2-D uniform instead for 3-D isotropic scattering environment). Like the exponential correlation, the correlation matrix of the Bessel correlation model is also positive semidefinite. (The proof follows the same lines as for the correlation case using Theorem 2 in [16]). Yet unlike (6) that can be used to model correlation in dense or sparse scattering environment by adjusting the decorrelation distance x_0, (7) is a reasonable model for only dense scattering environment.

4. PERFORMANCE METRICS AND EVALUATIONS

In order to evaluate the impacts of correlations on multi-antenna systems, we need to choose certain performance metrics first. In this section, we use diversity gain [1], diversity measure [17], MIMO capacity [21] and throughput [23] as performance metrics.

4.1. Diversity Gain

For an N-port antenna in a Rayleigh-fading environment, the correlation matrix is

$$\mathbf{R} = E\left[\mathbf{h}\mathbf{h}^H\right] \tag{8}$$

where $\mathbf{h}$ is the column-vector diversity channel including the overall antenna effect, superscript H the Hermitian operator, and E the expectation. The output power of the MRC combiner is $P_{MRC} = \mathbf{h}^H\mathbf{h}$. Assuming independent, identically distributed (i.i.d.) Gaussian noises with unity variance, P_{MRC} then equals in value to the instantaneous signal-to-noise ratio (SNR), denoted as γ. The diversity gain (DG) is defined as the output SNR of a diversity antenna relative to that of a single ideal (i.e., with 100% total radiation efficiency) antenna at 1% outage probability level [1],

$$DG = F^{-1}(\gamma)/F_{ideal}^{-1}(\gamma)\big|_{1\%} \tag{9}$$

where $(\cdot)^{-1}$ denotes the functional inversion, F the cumulative distribution function of the MRC output SNR, and $F_{ideal}(\gamma) = 1 - \exp(-\gamma)$ the CDF of the output SNR of the ideal reference antenna in the Rayleigh fading environment.

To examine the effect of the correlation on the DG, we define the DG degradation as the ratio of DG in the presence of correlation to the DG in the i.i.d. channel case. Figure 2 shows the DG degradation for the special cases of positive and negative uniform correlations among antenna ports, respectively. Note that the assumption of a uniform correlation of -0.3 is valid up to four-port antenna only due to (5). It can be seen that the DG degradation due to the uniform correlation is larger for the diversity antenna with more ports and that the negative correlation causes more DG degradation than the positive correlation. Hence, the phase of the correlation also affects the diversity performance.

Before giving an explanation of this, we show first that, for a two-port antenna ($N = 2$), the DG depends only on the magnitude of the correlation: In a two-port antenna, the CDF of the MRC output SNR reduces to [8]

$$F(\gamma) = 1 - \frac{\lambda_1 \exp(-\gamma/\lambda_1) - \lambda_2 \exp(-\gamma/\lambda_2)}{\lambda_1 - \lambda_2}. \tag{10}$$

It was shown in [8] that (10) converges to the true value as $\lambda_i \to \lambda$ ($i = 1, 2$). The eigenvalues of the covariance matrix

$$\mathbf{R} = \begin{bmatrix} 1 & \rho \\ \rho^* & 1 \end{bmatrix} \tag{11}$$

are

$$\lambda_1 = 1 + |\rho|, \quad \lambda_2 = 1 - |\rho|. \tag{12}$$

Combining (9), (10), and (12), it follows that the DG of the two-port antenna depends only on the correlation magnitude. This implies that, for mobile handset antenna that has only two antenna ports, it is sufficient to characterize its correlation by the correlation magnitude (or envelop or power correlation).

We resort to majorization theory [17] to show why the phase of the correlation affects the DG for antennas with more than two ports: For two real-valued $M \times 1$ vectors $\mathbf{a}$ and $\mathbf{b}$ in descending order,

$\mathbf{a}$ majorizes $\mathbf{b}$, denoted as $\mathbf{a} \succ \mathbf{b}$, if $\sum_{i=1}^{m} a_i \geq \sum_{i=1}^{m} b_i$ $(m = 1, \ldots, M-1)$ and $\sum_{i=1}^{M} a_i = \sum_{i=1}^{M} b_i$. Assume that $\mathbf{a}$ and $\mathbf{b}$ are two eigenvalue vectors associated with correlation matrices $\mathbf{R}_a$ and $\mathbf{R}_b$, $\mathbf{R}_a$ is more correlated than $\mathbf{R}_b$ if $\mathbf{a} \succ \mathbf{b}$. For two correlation matrices with the same correlation magnitudes but different correlation phases, their eigenvalue vectors are different. Note that throughout this paper without loss of generality eigenvalue vectors are assumed to be in descending order. For better illustration, we give a numerical example next: For a correlation matrix of a four-port antenna with uniform correlation of 0.3,

$$\mathbf{R}_a = \begin{bmatrix} 1 & 0.3 & 0.3 & 0.3 \\ 0.3 & 1 & 0.3 & 0.3 \\ 0.3 & 0.3 & 1 & 0.3 \\ 0.3 & 0.3 & 0.3 & 1 \end{bmatrix}, \tag{13}$$

the eigenvalue vector is $\mathbf{a} = [1.9\ 0.7\ 0.7\ 0.7]^T$; for a correlation matrix of a four-port antenna with uniform correlation of -0.3,

$$\mathbf{R}_b = \begin{bmatrix} 1 & -0.3 & -0.3 & -0.3 \\ -0.3 & 1 & -0.3 & -0.3 \\ -0.3 & -0.3 & 1 & -0.3 \\ -0.3 & -0.3 & -0.3 & 1 \end{bmatrix}, \tag{14}$$

the eigenvalue vector is $\mathbf{b} = [1.3\ 1.3\ 1.3\ 0.1]^T$. Hence, $\mathbf{a} \succ \mathbf{b}$ and $\mathbf{R}_b$ are more correlated than $\mathbf{R}_a$. This explains why the DG of a four-port antenna with a uniform correlation of -0.3 is smaller than that with a uniform correlation of 0.3 (see Figure 2).

Note that a uniform correlation of -0.3 has been observed in a practical four-port antenna [14]. Nevertheless, it might be impractical to design a large array (with many elements) that has uniform correlation. That is why our simulation for the uniform correlation has been limited up to four-port antennas.

For antennas with more ports, we resort to exponential and Bessel correlations by assuming uniform rectangular arrays (URA) with a fixed inter-element spacing of half-wavelength. Figure 3 shows the diversity degradations of various URA sizes for both exponential and Bessel correlations. Note that for fair comparison of the two correlation models, the decorrelation distance in (6) is set to half-wavelength (cf. Section 3). It can be seen that the Bessel correlation causes more degradation than the exponential correlation; yet for both models the diversity gain performance improves as the number of antennas increases (i.e., as the array size increases with a fixed inter-element separation).

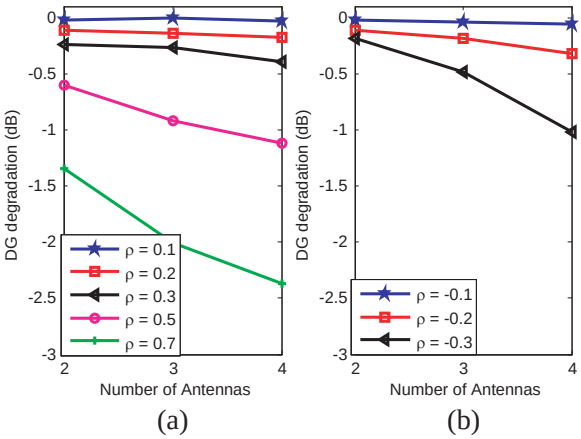

Figure 2. DG degradation due to uniform correlation. (a) Graph corresponds to positive correlation; (b) graph corresponds to negative correlation.

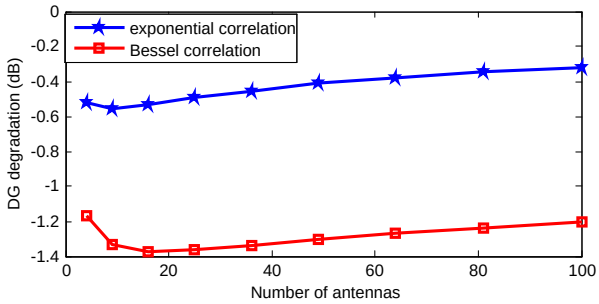

Figure 3. DG degradations due to exponential and Bessel correlations for half-wavelength inter-element spacing and decorrelation distance.

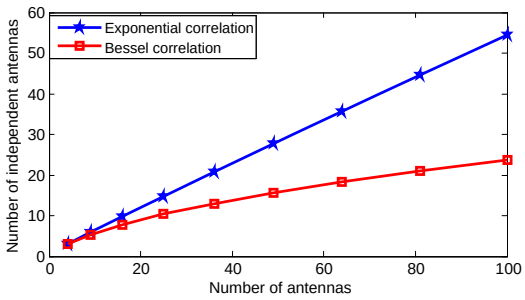

Figure 4. Numbers of independent antennas for exponential and Bessel correlations.

4.2. Diversity Measure

In contrast to the popular diversity gain, there is an easier way to characterize the diversity performance. That is diversity measure [17]

$$N_{ind} = \left(\frac{tr(\mathbf{R})}{\|\mathbf{R}\|_F} \right)^2 \tag{15}$$

where $tr(\cdot)$ is trace operator, and the subscript F denotes Frobenius norm. The diversity measure is simply the number of independent antennas. Actually, it has been used for estimating independent sample number in RC measurements [18–20].

For evaluating the correlations of two-port antennas, it is sufficient to compare the correlations of different antennas in that each two. However, for antennas with more than two ports, multiple correlations exist between the antenna ports. One may use the majorization theory to compare the correlations of two arrays with the same number of antenna ports. Yet a simpler way is to use the diversity measure. Assume URA with a fixed inter-element spacing (and decorrelation distance) of half-wavelength. Figure 4 shows the diversity measures (or independent antenna numbers) of different array sizes under exponential and Bessel correlations. It can be seen that the exponential correlation results in less correlated correlation matrix (and therefore more independent antenna number) than the Bessel correlation. This implies massive MIMO results obtained by assuming exponential correlation may be optimistic.

4.3. Capacity and Throughput

Capacity is the theoretically maximum achievable data rate. To achieve the capacity, the input signal needs to be Gaussian distributed [22] and the MCS should have an infinitesimal granularity in order to support any data rate that is matched with the fading channel. As a result, capacity is usually not achievable in practical systems. Nevertheless, we still characterize the MIMO system using it in this paper in that it is the most popular MIMO performance metric [2, 3, 8, 11, 12].

The instantaneous capacity (or strictly speaking mutual information) of a MIMO system, where only the receiver knows the channel state information (i.e., open-loop MIMO system), is, e.g., [11]

$$C = \log_2 \left[\det \left(\mathbf{I} + \frac{\gamma_0}{N_t} \mathbf{H}\mathbf{H}^H \right) \right] \tag{16}$$

where $\mathbf{I}$ is the identity matrix, det the determinant, $\log_2$ the logarithm to the base 2, γ_0 the average SNR per receive antenna, and $\mathbf{H}$ the MIMO channel matrix.

To illustrate the correlation phase effect on MIMO capacity, we assume a 4×4 MIMO system, where the transmit antennas are uncorrelated, whereas the receive antennas have uniform correlations of 0.3 and -0.3 [i.e., (13) and (14)], respectively. Figure 5 shows the ergodic capacity (i.e., the average of the instantaneous mutual information) as well as the CDF of the instantaneous capacity. As can be seen, the uniform correlation of -0.3 yields a worse MIMO capacity performance than that of the uniform correlation of 0.3; and the difference is more noticeable at high SNR. Note that the capacity-achieving system allows adaptive transmission of arbitrary streams according to the instantaneous

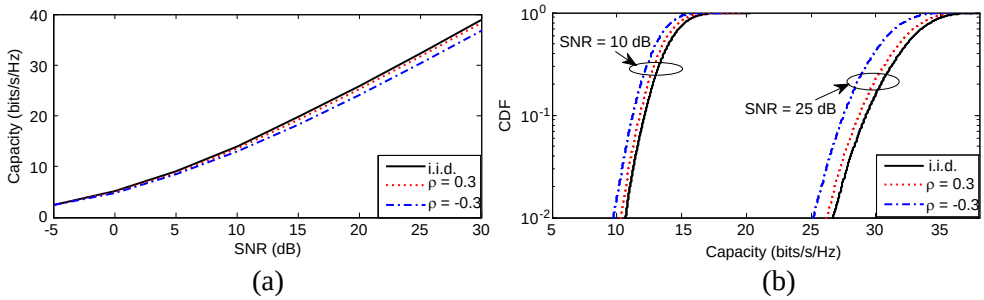

Figure 5. (a) Ergodic capacity and (b) CDF of the instantaneous capacity of a 4×4 open-loop MIMO system.

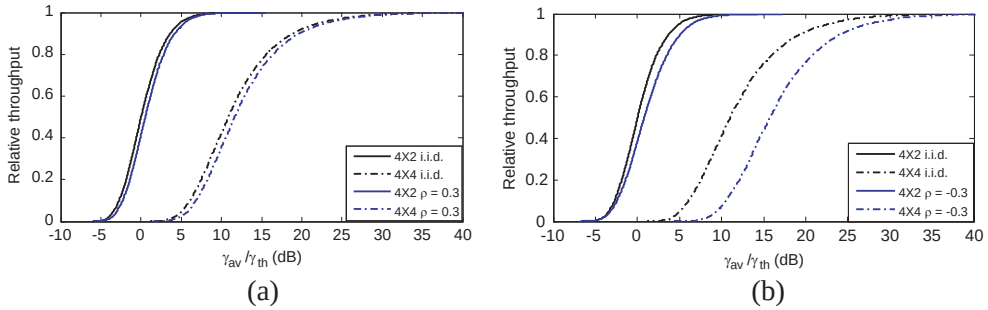

Figure 6. Relative throughput of 4×2 and 4×4 MIMO systems with full spatial multiplexing gains. (a) Graph corresponds to the uniform correlation of 0.3; (b) graph corresponds to the uniform correlation of -0.3. Note that for a fixed MCS the (absolute) throughput of the 4×4 system is twice of that of the 4×2 system. However, their relative throughputs (i.e., probabilities of detecting 4 and 2 data streams) are both normalized to one.

channel condition, e.g., in a rank-deficient MIMO channel the capacity is achieve by a combination of spatial multiplexing and diversity by transmitting less than four streams (each stream with arbitrary payload). Therefore, the correlation effect on the capacity is less profound than that on the throughput with fixed MCS and number of streams (cf. Section 2.2). Nevertheless, it is shown again that the phase of the correlation affects the MIMO performance.

Unlike capacity, throughput is the actual data rate that can be achieved by practical wireless systems. A simple throughput model has been presented in [23], based on which, the average throughput of a system with fixed MCS in a fading channel can be approximated by

$$T_{put}\left(\bar{\gamma}\right) = T_{put,\max}\left(1 - F(\gamma_{th}/\bar{\gamma})\right) \tag{17}$$

where $\bar{\gamma}$ represents the average γ, γ_{th} is the threshold value, F denotes the CDF of γ, and $T_{put,\max}$ denotes the maximum data rate. We define the relative throughput as $T_{put}/T_{put,\max}$ and use the relative throughput hereafter.

For simplicity, we assume open-loop MIMO systems with zero-forcing (ZF) receivers and that the transmit antennas are uncorrelated. The MIMO channel then can be modeled as

$$\mathbf{H} = \mathbf{R}^{1/2}\mathbf{H}_w \tag{18}$$

where $\mathbf{H}_w$ denotes the spatially white MIMO channel with i.i.d. and unit variance complex Gaussian variables, and $\mathbf{R}^{1/2}$ is the (Hermitian) square root of $\mathbf{R}$. For simplicity and without loss of generality, we assume unity input signal power and noise variance, the SNR of the ith stream is then [21]

$$\gamma_i = 1 \Big/ \left[\left(\mathbf{H}^H\mathbf{H}\right)^{-1}\right]_{i,i} \tag{19}$$

where $[\mathbf{X}]_{i,i}$ denotes the ith diagonal element of the matrix $\mathbf{X}$.

Figure 6 shows the relative throughputs of 4×2 and 4×4 open-loop MIMO systems with ZF receivers supporting 2 and 4 data streams (with and without correlation), respectively. We see that a small uniform correlation of -0.3 degrades the 4×2 throughput by about 1 dB (i.e., it needs 1 dB more power to achieve the same throughput as in i.i.d. channel case); but the same correlation of -0.3 will degrades the 4×4 MIMO systems by about 5 dB. On the other hand, a uniform correlation of the same magnitude but with opposite phase, i.e., 0.3, results in negligible throughput performance degradations. This can be explained intuitively: the eigenvalues of the correlation matrix with uniform correlation of -0.3 are 1.3, 1.3, 1.3, and 0.1, whereas the eigenvalues of the correlation matrix with uniform correlation of 0.3 are 1.9, 0.7, 0.7, 0.7; and it is the smallest eigenvalue of 0.1 that makes it difficult to detect the fourth data stream, implying a worse throughput performance for the 4×4 MIMO system with full spatial multiplexing. For the 4×2 MIMO system with full spatial multiplexing, the throughput performance degradation of the uniform correlation of -0.3 is not severe because the best two eigenvalues ensure the reliable transmission of the two streams.

Comparing Figures 2 and 6, it seems that the correlation (e.g., the uniform correlation of -0.3) may have a much more profound effect on the throughput performance than that on the diversity performance. This is because it suffices to have one large enough eigenvalue for the diversity techniques to work (since the diversity techniques handle only one stream); for the spatial multiplexing, it is vital to have M strong enough eigenvalues in order to support the transmission of M streams.

5. MEASUREMENTS

The reverberation chamber (RC) has been used for various measurements of wireless devices due to its convenience and measurement repeatability [24–27]. In this paper, we use the RC measurement for studying the effects of antenna correlations. The RC is basically a metal cavity with many excited modes which are stirred to create an isotropic rich scattering environment. The RC used in this work has a size of $1.75 \times 1.25 \times 1.8\,\mathrm{m}^3$. Figure 7 shows a drawing of the RC: it is equipped with two plate stirrers, a turn-table platform (on which the antenna under test is mounted), and three wideband antennas (mounted on three orthogonal walls with different polarizations inside the chamber). We hereafter refer to these three antennas as wall antennas. Note that the wall antennas need not to be in the RC's working volume; whereas the antenna under test (AUT) must be in the working volume, where the field uniformity is guaranteed. In this work, the AUT is a compact wideband four-port Bowtie antenna [14]; and it was placed on the turn-table platform (which is in the working volume) during the measurement. In the measurements, the platform was moved to 20 positions spaced by 18° and at each platform position each of the two plates move simultaneously to 10 positions. At each stirrer position and for each of the three wall antennas a full frequency sweep was performed by a vector network analyzer (VNA) and the S-parameter S_{21} between the wall antennas and each port of the Bowtie antenna were recorded. Using the jargon of communications S_{21} is the channel transfer function, which is random due to the mode stirring in the RC.

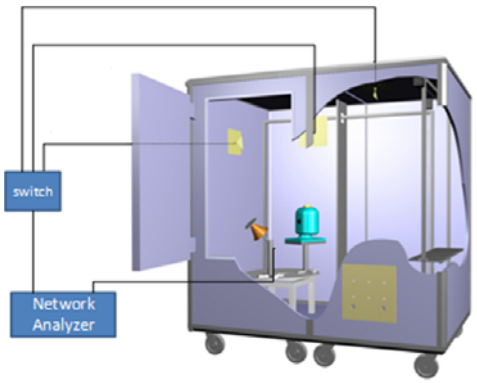

Figure 7. Drawing of the RC.

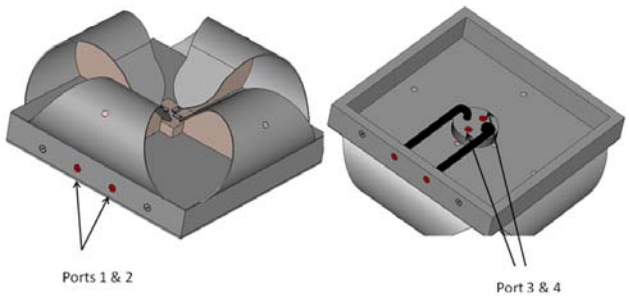

Figure 8. CST model of the bowtie antenna.

Figure 8 shows a model of the Bowtie antenna in CST. It was designed to cover the frequency range of 1.7∼2.7 GHz. The 4 ports of the Bowtie antenna are marked in the figure. Due to the symmetry of the antenna, it is sufficient to present correlations between Ports 1 and 2, Ports 1 and 3, and Ports 1 and 4. From the CST simulation, we obtain embedded radiation patterns of the Bowtie antenna, from which we can calculate the correlations using (2). From RC measurement, we obtain the samples of the channel transfer function (i.e., S_{21}) from which we can calculate the correlations using (1), where the X_m is S_{21} seen at the mth port of the Bowtie antenna. Note that the expectation in (1) is approximated by averaging the 600 samples (20 platform positions $\times$10 plate positions $\times$3 wall antennas) of S_{21}. Figure 9 shows the correlations calculated from the simulated antenna patterns and the measured channels. It should be noted that due to manufacture tolerance and measurement uncertainty (it is difficult to measure small correlation accurately) the measured correlations slightly differ from the simulated ones. Nevertheless, from both CST simulation and RC measurement, it is evident that the Bowtie antenna has a uniform correlation (among antenna ports). This indicates that the uniform correlation does exist in practical antennas.

The measured correlation uncertainty has been experimentally characterized in [28], where it is concluded that the number of samples and the correlation level are the dominant contributions to the uncertainty of the measured correlation. The distribution of the estimated correlation coefficient using (1) is given by [29], based on which it is easy to derive the standard deviation (STD) of the measured correlation for a given expected real-valued ρ:

$$STD\left[\hat{\rho}\right] \approx \sqrt{\frac{(1-\rho^2)^2}{N}\left(1+\frac{11\rho^2}{2N}\right)} \tag{20}$$

where N is the number of samples. Since the Bowtie antenna's correlation ranging from -3.0 to -1.5 (over frequency) and $N = 600$, the variance of the measured correlation ranges approximately from 0.037 to 0.040. This uncertainty is certainly not enough to explain the discrepancy in Figure 9. Hence, it is believed that the measurement tolerance of the Bowtie antenna is the main reason of the discrepancy, given the fact that curves of the four bended petals of the manufactured Bowtie antenna has noticeable differences between each other and deviate from that of the model.

To further study the correlation effect on MIMO systems, MIMO LTE systems are measured in the RC. Note that due to practical measurement constraints (e.g., currently all available communication tester support only up to two antenna ports), throughput measurements are limited to 2×2 MIMO systems.

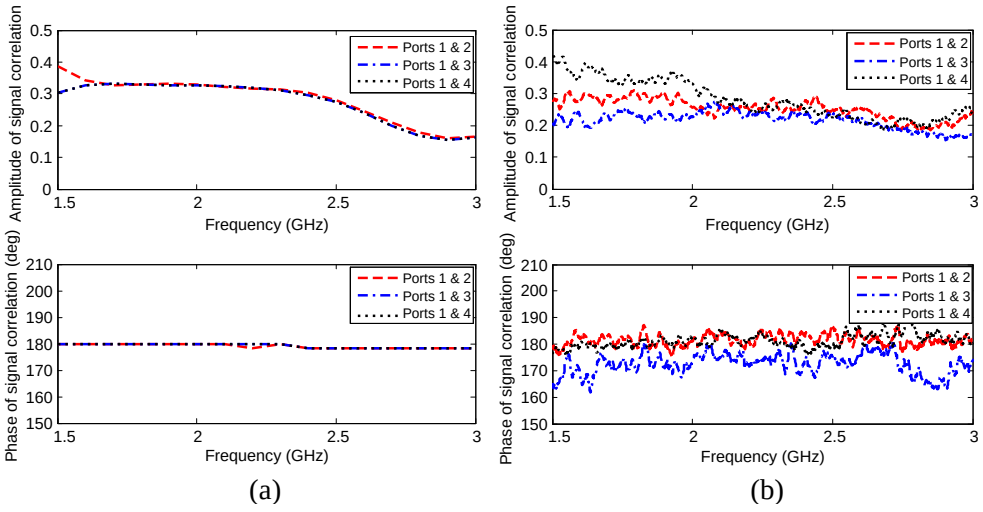

Figure 9. Amplitudes and phases of correlations of Bowtie antenna: (a) simulated correlations, i.e., correlations calculated from antenna patterns obtained from CST simulation; (b) measured correlations, i.e., correlations calculated from channel samples measured in the RC.

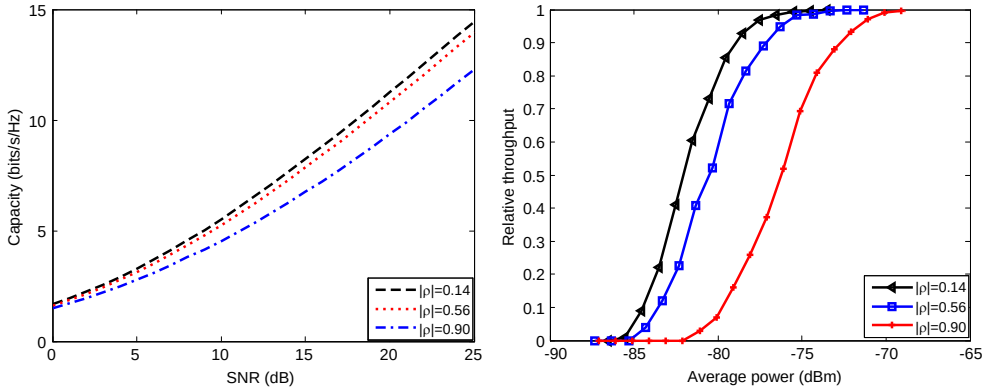

Figure 10. (a) Measured MIMO capacity of the CTIA reference antennas and (b) relative throughput of a LTE phone connected to the CTIA reference antennas.

A commercial communication tester is used as the LTE base station. The device under test (DUT) is a commercial LTE mobile phone with external antenna ports available for wireless testing. To introduce known antenna correlation in the throughput measurement, the DUT was connected with the two-port power-balanced good, nominal, and bad CTIA reference antennas [30] that were located inside the RC. Note that the CTIA reference antennas include RF shielding boxes in which DUT was placed. Measurements of DUT were performed on the LTE band 13, i.e., 751 MHz, with 10-MHz system bandwidth in closed-loop configuration. The LTE system was set to a fixed 64 QAM modulation with maximum rates of about 35 Mbps for the spatial multiplexing measurements. The magnitudes of the complex (antenna) correlation coefficients of the good, nominal, and bad CTIA reference antennas are about 0.14, 0.56, and 0.90, respectively. The CTIA reference antennas are power-balanced and the efficiencies of the good, nominal, and bad CTIA reference antennas are about -1.4, -3.1, and -4.0 dB, respectively. In order to focus on the correlation effect alone, we calibrated out the antenna efficiencies in post-processing of the measured data.

In addition, we performed passive measurement of the CTIA reference antennas as receive antennas in the RC, while using two uncorrelated RC wall antennas as transmit antennas. The ergodic MIMO capacity of the measured 2×2 MIMO channel is calculated and shown in Figure 10(a), whereas the measured relative throughput is shown in Figure 10(b). Note that only absolute power values are available from the testing instrument. Thus, the measured throughputs are shown as a function of the (received) average power. It can be seen that, even for the two-port antennas, the correlation has a much greater impact on the throughput than on the capacity (a correlation of 0.5 has negligible effect on capacity, whereas it degrades the throughput by approximately 2 dB); the effect of the correlation on capacity increases with increasing SNR, whereas the correlation's effect on the throughput is almost independent on the SNR (or received power). This implies that the rule-of-thumb of smaller than 0.5 correlation in magnitude is not a good criterion in MIMO antenna designs even for two-port antennas. In fact, a correlation no larger than 0.3 in magnitude is needed to ensure throughput degradation that is smaller than 0.5 dB [31].

6. CONCLUSION

This work revisits signal correlation and its effect on MIMO performances. In contrast to the common beliefs that the correlation magnitude of 0.5 is negligible for MIMO performance, we show that a correlation of 0.5 has noticeable impact on the throughput of a 2×2 MIMO LTE system (even though it does has little impact on the 2×2 MIMO capacity). Moreover, it is usually assumed that the correlation affects the MIMO performance only via its magnitude, it is found in this work that the latter is only true for two-port antennas; and in general the correlation's effect on the MIMO performances depends on its phase and the number of antennas. Correlations with the same magnitudes but different phases

may result in different MIMO performances, especially for the spatial multiplexing throughput. The paper justifies the uniform correlation assumption using a practical multi-port antenna as an example. In addition to the uniform correlation model, two more realistic correlation models are presented; and their feasibilities are analyzed.

APPENDIX A.

The spatial channel correlation without antenna effect can be calculated by

$$\rho = \int_0^{2\pi} \int_0^{\pi} \exp(jkd \sin\theta \cos\phi) p(\theta, \phi) d\theta d\phi \tag{A1}$$

where k is wave number, d is the separation between two (imaginary) isotropic antennas, ϕ and θ represents the azimuth and elevation angles, respectively, and $p(\theta, \phi)$ is their joint probability density function (PDF). In a 3-D isotropic scattering environment,

$$p(\theta, \phi) = \frac{\sin\theta}{4\pi} \quad (0 \le \theta < \pi, \quad 0 \le \phi < 2\pi) \tag{A2}$$

Substituting (A2) into (A1), the spatial correlation becomes

$$\rho = \frac{\sin(kd)}{kd} \tag{A3}$$

which is a sinc function.

APPENDIX B.

For the uniform correlation model, the correlation matrix of an N-port antenna becomes

$$\mathbf{\Phi} = \begin{bmatrix} 1 & \rho & \dots & \rho \\ \rho & 1 & \dots & \rho \\ \vdots & \vdots & \ddots & \vdots \\ \rho & \rho & \dots & 1 \end{bmatrix}. \tag{B1}$$

For $\mathbf{\Phi}$ to be positive semidefinite, it must satisfy

$$\mathbf{\Phi} = \mathbf{L}\mathbf{L}^T \tag{B2}$$

where $\mathbf{L}$ is real-valued matrix with proper dimensions. The actual entries of $\mathbf{L}$ depend not only on the value of ρ but also on the decomposition (or matrix square root). Several methods exist for the decomposition. Nevertheless, the feasibility of the correlation matrix should not depend on the decomposition method. Hence, we choose a simplest decomposition for (B1):

$$\mathbf{L} = \begin{bmatrix} a & b & \dots & b \\ b & a & \dots & b \\ \vdots & \vdots & \ddots & \vdots \\ b & b & \dots & a \end{bmatrix} \tag{B3}$$

where a and b are solutions for the following set of equations

$$\begin{aligned} a^2 + (N-1)b^2 &= 1 \\ 2ab + (N-2)b^2 &= \rho \end{aligned}. \tag{B4}$$

All the solutions to (B4) involve the square root of $(N-1)\rho+1$. Since a and b are real-valued, $(N-1)\rho+1$ should be no smaller than zero, i.e.,

$$\rho \ge -1/(N-1). \tag{B5}$$

REFERENCES

1. Schwartz, M., W. R. Bennet, and S. Stein, *Communication Systems and Techniques*, IEEE Press, 1996.
2. Levin, G. and S. Loyka, "From multi-keyholes to measure of correlation and power imbalance in MIMO channels: Outage capacity analysis," *IEEE Trans. Inf. Theory*, Vol. 57, No. 6, 3515–3529, Jun. 2011.
3. Chen, X., P.-S. Kildal, and J. Carlsson, "Revisiting the complex correlation in a MIMO system," *8th European Conference on Antennas and Propagation*, Hague, Netherlands, Apr. 6–11, 2014.
4. Gradoni, G., V. Mariani Primiani, and F. Moglie, "Reverberation chamber as a multivariate process: FDTD evaluation of correlation matrix and independent positions," *Progress In Electromagnetics Research*, Vol. 133, 217–234, 2013.
5. Grimmett, G. and D. Stirzaker, *Probability and Random Processes*, 3rd Edition, Oxford University Press, 2001.
6. Stein, S., "On cross coupling in multiple-beam antennas," *IRE Trans. Antennas Propagat.*, 548–557, Sep. 1962.
7. Janssen, N., K. A. Remley, C. L. Holloway, and W. F. Young, "Correlation coefficient and loading effects for MIMO antennas in a reverberation chamber," *EMC Europe*, 514–519, Brugge, Sep. 2–6, 2013.
8. Chen, X., P.-S. Kildal, J. Carlsson, and J. Yang, "MRC diversity and MIMO capacity evaluations of multi-port antennas using reverberation chamber and anechoic chamber," *IEEE Trans. Antennas Propag.*, Vol. 61, No. 2, 917–926, Feb. 2013.
9. Blanch, S., J. Romeu, and I. Corbella, "Exact representation of antenna system diversity performance from input parameter description," *Electronics Letters*, Vol. 39, No. 9, 705–707, May 2003.
10. Li, H., X. Lin, B. K. Lau, and S. He, "Equivalent circuit based calculation of signal correlation in lossy antenna arrays," *IEEE Trans. Antennas Propag.*, Vol. 61, No. 10, 5214–5222, Oct. 2013.
11. Chiani, M., M. Z. Win, and A. Zanella, "On the capacity of spatially correlated MIMO Rayleigh-fading channels," *IEEE Trans. Inf. Theory*, Vol. 49, No. 10, 2363–2371, Oct. 2003.
12. Chizhik, D., F. Farrokhi, J. Ling, and A. Lozano, "Effect of antenna separation on the capacity of BLAST in correlated channels," *IEEE Commun. Lett.*, Vol. 4, No. 11, 337–339, Nov. 2000.
13. Laub, A. J., *Matrix Analysis for Scientists and Engineers*, SIAM, Philadelphia, PA, 2005.
14. Kildal, P.-S., X. Chen, M. Gustafsson, et al., "MIMO characterization on system level of 5G micro base stations subject to randomness in LOS," *IEEE Access*, Vol. 2, 1062–1075, 2014.
15. Rappaport, T. S., *Wireless Communications — Principles and Practice*, 2nd Edition, Prentice Hall PTR, 2002.
16. Yaglom, A. M., *Theory of Stationary and Related Random Functions*, Springer, 1987.
17. Jorswieck, E. and H. Boche, "Majorization and matrix-monotone functions in wireless communications," *Foundations Trends Commun. Inf. Theory*, Vol. 3, No. 6, 553–701, 2006.
18. Chen, X., "On independent platform sample number for reverberation chamber measurements," *IEEE Trans. Electromagn. Compat.*, Vol. 54, No. 6, 1306–1309, Dec. 2012.
19. Chen, X., "Experimental investigation of the number of independent samples and the measurement uncertainty in a reverberation chamber," *IEEE Trans. Electromagn. Compat.*, Vol. 55, No. 5, 816–824, Oct. 2013.
20. Pirkl, R. J., K. A. Remley, and C. S. L. Patané, "Reverberation chamber measurement correlation," *IEEE Trans. Electromagn. Compat.*, Vol. 54, No. 3, 533–544, 2012.
21. Paulraj, A., R. Nabar, and D. Gore, *Introduction to Space-time Wireless Communication*, Cambridge University Press, 2003.
22. Cover, T. M. and J. A. Thomas, *Elements of Information Theory*, John Wiley & Sons, 1991.
23. Chen, X., P.-S. Kildal, and M. Gustafsson, "Characterization of implemented algorithm for MIMO spatial multiplexing in reverberation chamber," *IEEE Trans. Antennas Propag.*, Vol. 61, No. 8,

4400–4404, Aug. 2013.

24. Recanatini, R., F. Moglie, and V. Mariani Primiani, "Performance and immunity evaluation of complete WLAN systems in a large reverberation chamber," *IEEE Trans. Electromagn. Compat.*, Vol. 55, No. 5, 806–815, Oct. 2013.
25. Genender, E., C. L. Holloway, K. A. Remley, J. M. Ladbury, G. Koepke, and H. Garbe, "Simulating the multipath channel with a reverberation chamber: Application to bit error rate measurements," *IEEE Trans. Electromagn. Compat.*, Vol. 52, 766–777, 2010.
26. Im, Y.-T., M. Ali, and S.-O. Park, "Slow modulation behavior of the FMCW radar for wireless channel sounding technology," *IEEE Trans. Electromagn. Compat.*, Vol. 56, No. 5, 1229–1237, 2014.
27. Ferrara, G., M. Migliaccio, and A. Sorrentino, "Characterization of GSM non-line-of-sight propagation channels generated in a reverberating chamber by using bit error rates," *IEEE Trans. Electromagn. Compat.*, Vol. 49, No. 3, 467–473, Aug. 2007.
28. Chen, X., P.-S. Kildal, and J. Carlsson, "Measurement uncertainties of capacities of multi-antenna system in anechoic chamber and reverberation chamber," *8th International Symposium on Wireless Communication Systems*, 216–220, Aachen, Germany, Nov. 6–9, 2011.
29. Olkin, I. and J. W. Pratt, "Unbiased estimation of certain correlation coefficients," *The Annals of Mathematical Statistics*, Vol. 29, No. 1, 201–211, 1958.
30. Szini, I., "Reference antenna proposal for MIMO OTA," *CTIA Contribution MOSG110504R1*, May 2011.
31. Chen, X., "Throughput multiplexing efficiency for MIMO antenna characterization," *IEEE Antennas Wireless Propag. Lett.*, Vol. 12, 1208–1211, 2013.